Heterotrimetallic Complexes $[\{Pt(RNH_2)_2(\mu\text{-}NHCOtBu)_2\}_2M](ClO_4)_n$ (M = Mn, Co, Cu, Ni, Cd, and Zn, n = 2; M = In, n = 3), $[\{Pt(NH_3)(\mu\text{-}DACHCOtBu)(\mu\text{-}NHCOtBu)\}_2Ni](ClO_4)_2$, and $[\{Pt(RNH_2)_2(NHCOtBu)_2\}_3Ag_3](ClO_4)_3$ Bridged by Amidate Ligands: A Novel Amidate−Amine Interligand Reaction During the Pt−Ni Bond Formation

Wanzhi Chen,[a] Fenghui Liu,[a] Takuya Nishioka,[a] and Kazulo Matsumoto*[a]

Keywords: Platinum / Amidate ligand / Metal−metal interaction / Heterotrimetallic complexes / Nickel

The neutral square-planar complexes $[Pt(NH_2CH_2CH_2OCH_3)_2(NHCOtBu)_2]$, $[Pt(DACH)(NHCOtBu)_2]$ (DACH = *trans*-1,2-diaminocyclohexane), and $[Pt(NH_2CH_2CH_2NMe_2)(NHCOtBu)_2]$ have been prepared by hydrolysis of the corresponding $[Pt(RNH_2)_2(NCtBu)_2](ClO_4)_2$ with NaOH. Reactions of $[Pt(RNH_2)_2(NHCOtBu)_2]$ with metal ions afforded Pt–M–Pt clusters $[\{Pt(RNH_2)_2(\mu\text{-}NHCOtBu)_2\}_2M](ClO_4)_n$ (M = Mn, Co, Cu, Ni, Cd, Zn, and In; n = 2 or 3) and $[\{Pt(NH_2CH_2CH_2NMe_2)(\mu\text{-}NHCOtBu)_2\}_2M](ClO_4)_2$ (M = Co, Ni). The Pt_2M (M = Mn, Co, Cu, Ni, Zn, and In) complexes consist of a linear Pt–M–Pt core bridged by four pivalamidate ligands. The Pt–M–Pt angles are 180° or nearly so. The central metal ions with an octahedral geometry are coordinated by four equatorial amidate oxygen atoms and two platinum atoms occupy the axial site. One of the two *t*-BuCO group shifts to the neighboring nitrogen atom of DACH (DACH = *trans*-1,2-diaminocyclohexane) in the reaction of $[Pt(DACH)(NHCOtBu)_2]\cdot 4H_2O$ with Ni^{2+} to generate the unexpected $[\{Pt(NH_3)(DACHCOtBu)(\mu\text{-}NHCOtBu)\}_2Ni](ClO_4)_2$. The central Cd ion in $[\{Pt(RNH_2)_2(\mu\text{-}NHCOtBu)_2\}_2Cd](ClO_4)_2$ is trigonal-bipyramidal and the Pt–Cd–Pt is bent. Treatment of $[Pt(NH_2CH_2CH_2OCH_3)_2(NHCOtBu)_2]$ with an equimolar amount of $AgClO_4$ yielded the Pt_4Ag_3 cluster consisting of alternate Pt and Ag atoms either doubly or singly bridged by amidate ligands. The spectroscopic and electrochemical studies show that the metal–metal interactions between platinum and the heterometal ions are very weak.

Introduction

Heteronuclear metal complexes of linearly arranged metal arrays with metal−metal bonds may act as multifunctional catalysts for organic transformation processes and multifunctional materials with versatile physical and chemical properties.[1−6] Heterometallic cluster systems involving platinum(II) and other metal ions of d^{10} and s^2 electronic configuration exhibit unique physicochemical properties such as luminescence based on the d^8 and the closed-shell metal−metal interactions, and have potential applications in chemical devices. The metallophilic interactions are important in determining the solid-state structures and also contribute to the properties of such complexes in solution. Many complexes containing Pt−M bonds, such as $Pt^{II}-Cu^{I}$,[3,4] $Pt^{II}-Cd^{II}$,[7] and $Pt^{II}-Tl^{I}$,[2,7−9] display intense luminescence that is correlated with the metal−metal bonds through metallophilic interactions.[10]

We have found that amidate-bridged dimeric Pt^{III} complexes are efficient catalysts for the epoxidation and dihydroxylation of olefins and can activate the C−H bonds of ketones.[11] The versatile role of transition metal ions of the first row in many organic oxidation reactions suggests it would be of interest to prepare amidate-bridged heterometallic complexes having various Pt−M bonds.

The electron-rich platinum atom in $[Pt(RNH_2)_2(NHCOR')_2]$ can act as a soft base through donating its d_{z^2} electrons to transition metal ions to form Pt−M bonds. Heterometallic Pt−M (M = Mn, Co, Ni, Cu) complexes are potentially useful reagents or catalysts for some organic oxidation processes since the role of these metals in oxidation reactions is well known. Few examples of symmetrical heterotrinuclear Pt−M−Pt complexes have been reported.[2,6] We reported recently that reactions of $[Pt(NH_3)_2(NHCOtBu)_2]$ with M^{2+} (M = Mn, Fe, Co, Ni, and Cu) ions afforded trinuclear complexes $[\{Pt(NH_3)_2(NHCOtBu)_2\}_2M]^{n+}$ exclusively.[6] The present work examines how different substituents on the amine ligands alter the metal−metal interactions and the possibility of obtaining new cluster compounds by introducing additional functional groups such as MeO and Me_2N. The

[a] Department of Chemistry, Advanced Research Institute of Science and Engineering, Waseda University,
Okubo, Shinjuku-Ku 169-8555, Tokyo, Japan
Fax: (internat.) + 81-3/5273-3489
E-mail: kmatsu@waseda.jp

  DOI: 10.1002/ejic.200200684

compound $[Pt(RNH_2)_2(NHCOR')_2]$ is expected to have better donating abilities than $[Pt(NH_3)_2(NHCOR')_2]$. To further investigate such metal−metal bonds, we describe herein the synthesis and structural characterization, including X-ray diffraction analysis, of the trinuclear complexes $[\{Pt(DACH)(\mu\text{-}NHCOtBu)_2\}_2M](ClO_4)_n$ (M = Cu, Co, Mn, and Cd, n = 2; M = In, n = 3), $[\{Pt(\mu\text{-}DACHNHCOtBu)(\mu\text{-}NHCOtBu)\}_2Ni](ClO_4)_2$, $[\{Pt(NH_3)_2(\mu\text{-}NHCOtBu)_2\}_2M](ClO_4)_n$ (M = Cd, n = 2; M = In, n = 3), $[\{Pt(NH_2CH_2CH_2NMe_2)(\mu\text{-}NHCOtBu)_2\}_2M](ClO_4)_2$ (M = Co, Ni), $[\{Pt(NH_2CH_2CH_2OCH_3)_2(\mu\text{-}NHCOtBu)_2\}_2M](ClO_4)_2$ (M = Co, Zn), and heptanuclear $[\{Pt(NH_2CH_2CH_2OCH_3)_2(\mu\text{-}NHCOtBu)_2\}_4Ag_3](ClO_4)_2\cdot 2H_2O$. The electrochemistry of the trinuclear heterometallic complexes as well as their parent platinum complexes has also been studied.

Results and Discussion

Synthesis and Spectroscopic Characterization

The complexes synthesized are depicted in Schemes 1−3. $[Pt(DACH)(NHCOtBu)_2]$ (**2**), $[Pt(NH_2CH_2CH_2OCH_3)_2(NHCOtBu)_2]$ (**3**), and $[Pt(NH_2CH_2CH_2NMe_2)(NHCOtBu)_2]$ (**4**) were easily prepared by basic hydrolysis of the corresponding $[Pt(RNH_2)_2(NCtBu)_2]^{2+}$ in good yields.[12] The heteronuclear complexes **5**−**17** were readily obtained by mixing $[Pt(RNH_2)_2(NHCOtBu)_2]$ and the corresponding metal salts in water or water/acetone. Regardless of the Pt/M ratio used, the trinuclear Pt_2M (M = Mn, Co, Ni, Cu, Zn, Cd, and In) complexes were exclusively obtained in high yields. Attempts to prepare dimeric Pt−M complexes by using a large excess of M ions were unsuccessful. All the compounds were characterized by elemental analyses.

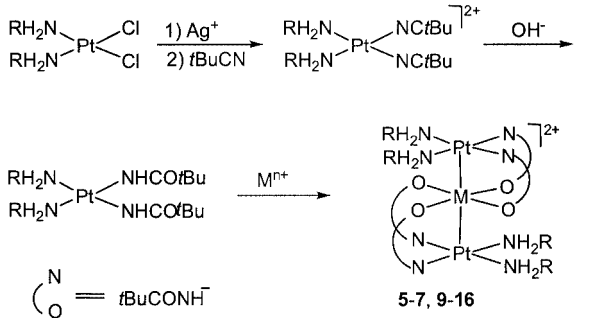

5, RNH_2 = 1/2 DACH, M = Mn^{2+}
6, RNH_2 = 1/2 DACH, M = Co^{2+}
7, RNH_2 = 1/2 DACH, M = Cu^{2+}
9, RNH_2 = 1/2 DACH, M = In^{3+}
10, RNH_2 = 1/2 DACH, M = Cd^{2+}
11, RNH_2 = NH_3, M = In^{3+}
12, RNH_2 = NH_3, M = Cd^{2+}
13, RNH_2 = 1/2 $NH_2CH_2CH_2NMe_2$, M = Co^{2+}
14, RNH_2 = 1/2 $NH_2CH_2CH_2NMe_2$, M = Ni^{2+}
15, RNH_2 = $NH_2CH_2CH_2OCH_3$, M = Zn^{2+}
16, RNH_2 = $NH_2CH_2CH_2OCH_3$, M = Co^{2+}

Scheme 1

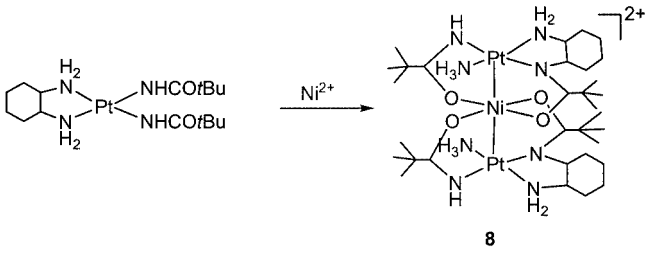

Scheme 2

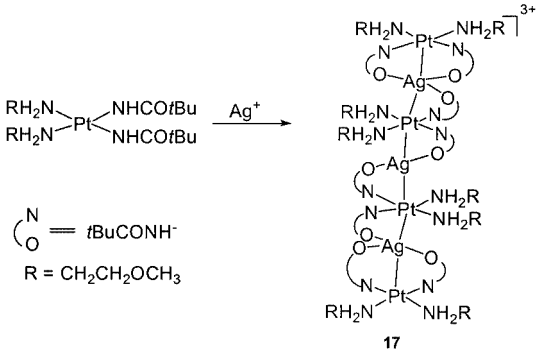

Scheme 3

The reaction of $[Pt(DACH)(NHCOtBu)_2]$ (**2**) and Ni^{2+} under the same conditions did not afford the expected Pt−Ni−Pt complex $[\{Pt(DACH)(\mu\text{-}NHCOtBu)_2\}_2Ni]^{2+}$, but, instead, $[\{Pt(NH_3)(\mu\text{-}DACHCOtBu)(\mu\text{-}NHCOtBu)\}_2Ni]^{2+}$ (**8**) through migration of a BuCO group to the DACH ligand (Scheme 2).

The oligomeric Pt_4Ag_3 complex $[\{Pt(NH_2CH_2CH_2OCH_3)_2(\mu\text{-}NHCOtBu)_2\}_4Ag_3](ClO_4)_2\cdot 2H_2O$ (**17**) was isolated as colorless crystals when $[Pt(NH_2CH_2CH_2OCH_3)_2(NHCOtBu)_2]$ was treated with 1 equiv. of $AgClO_4$ in water (Scheme 3). The compound is moderately soluble in acetone and ethanol and is light-sensitive. Silver(I) tends to form platinum(II)−silver(I) coordination polymers, which have been studied.[13,14]

The ^{195}Pt NMR resonances of $[Pt(DACH)(NCtBu)_2](ClO_4)_2$ (**1**) and $[Pt(DACH)(NHCOtBu)_2]$ (**2**) in [D_6]acetone appear at δ = −2857 and −2625 ppm as singlets, respectively, which are typical for a PtN_4 coordination sphere.[12,15] Both the ^1H NMR spectra of $[\{Pt(DACH)(\mu\text{-}NHCOtBu)_2\}_2In](ClO_4)_3\cdot(CH_3)_2CO$ (**9**) and $[\{Pt(DACH)(\mu\text{-}NHCOtBu)_2\}_2Cd](ClO_4)_2$ (**10**) in [D_6]DMSO show two sets of signals corresponding to the NH protons of amidate ligands, and four sets of signals each corresponding to two NH_2 protons of *trans*-1,2-diaminocyclohexane, respectively, indicating that these protons are magnetically unequal. Simultaneously, the ^1H NMR spectra exhibit two singlets (1:1) assigned to *t*Bu protons for **10**. Singlets at δ = −2429 (**9**) and −2562 ppm (**10**) appear in their ^{195}Pt NMR spectra. The ^1H NMR spectrum of $[\{Pt(NH_3)_2(\mu\text{-}NHCOtBu)_2\}_2In]^{3+}$ (**11**) consists of singlets at δ = 6.46, 4.12, 2.06, and 1.10 ppm assignable to NH, NH_3, $(CH_3)_2CO$, and *t*Bu, respectively. The ^1H NMR spectrum of $[\{Pt(NH_3)_2(\mu\text{-}NHCOtBu)_2\}_2Cd](ClO_4)_2$ (**12**) exhib-

its signals at δ = 5.42, 4.51, and 1.06 ppm due to NH_3, NH, and *t*Bu groups. The ^{195}Pt NMR spectra of **11** and **12** show singlets at δ = −2474 and −2561 ppm, respectively. No Pt−Cd coupling was observed. For comparison, the ^{195}Pt resonance of the starting compound $[Pt(NH_3)_2(NHCOtBu)_2]\cdot 2H_2O$ appears at δ = −2428 ppm in [D_6]DMSO. The change in chemical shifts of NH and NH_3 between complexes **11**, **12**, and $[Pt(NH_3)_2(NHCOtBu)_2]$ is clearly due to the complexation of Pt. Spin−spin coupling between ^{195}Pt and ^{113}Cd was not observed for the two cadmium complexes, probably because the interaction between the two metals is too weak. The small variation in ^{195}Pt chemical shifts compared to their parent platinum complexes suggests that the metal−metal interactions are weak in **9**−**12**.

The IR spectra of the trinuclear Pt_2M complexes **5**−**16** are very similar to their parent platinum compounds. There are two bands at $\tilde{\nu}$ = 3400 and 3245 cm^{-1} assignable to ν(N−H) of amine and amidate groups, respectively. The amidate bands at $\tilde{\nu}$ = 1556 ($[Pt(NH_3)_2(NHCOtBu)_2]$), 1562 (**2**), 1568 (**3**), and 1560 cm^{-1} (**4**) are assignable to the carbonyl stretching of the amidate ligands and are in the typical range of amidate anions. The δ(N−H) bands appear as shoulder peaks at $\tilde{\nu} \approx 1600$ cm^{-1}. The amide vibrations are only slightly shifted due to the complexation of the transition metal ions, and appear in the narrow range $\tilde{\nu}$ = 1562−1569 cm^{-1}. The carbonyl stretching band of the oligomeric Pt−Ag complex **17** shifts to a lower wavenumber, $\tilde{\nu}$ = 1531 cm^{-1}, showing enhanced electron delocalization within the amidate group. The skeletal vibrations at $\tilde{\nu}$ = 1481−1490 cm^{-1} and δ(NCO) bands at $\tilde{\nu} \approx 600$ cm^{-1} of $[Pt(RNH_2)_2(NHCOtBu)_2]$ complexes are essentially unaffected by heterometal coordination. These observations are consistent with the reported amidate complexes.[14]

Structure of $[\{Pt(RNH_2)(\mu\text{-}NHCOtBu)_2\}_2M](ClO_4)_2$ (M = Mn, Co, and Cu)

A few trimeric Pt_2M complexes derived from $[Pt(NH_3)_2(NHCOtBu)_2]$ have been described.[6] The compounds $[\{Pt(DACH)(\mu\text{-}NHCOtBu)_2\}_2M]^{2+}$ (M = Mn, **5**; Co, **6**, Cu **7**), $[\{Pt(NH_2CH_2CH_2NMe_2)(\mu\text{-}NHCOtBu)_2\}_2Co]^{2+}$ (**13**), and $[\{Pt(NH_2CH_2CH_2OCH_3)_2(\mu\text{-}NHCOtBu)_2\}_2Co]^{2+}$ (**16**) have essentially the same structures (Figures 1−5), and are discussed together below. Selected bond lengths and bond angles are given in Table 1. Overall, despite the different space groups, compounds **5**−**7**, **13**, and **16** have essentially the same structure, which consists of the trimetallic Pt−M−Pt (M = Mn, Co, and Cu) cations. Within the cations the heterometal ions are located at the center, and the three metal atoms are held together through Pt−M interactions and four bridging pivalamidate ligands. The Pt−N distances range from 1.985(8) to 2.052(10) Å, which are normal. The N−Pt−N angles indicate that the geometry about the platinum atom is square-planar. The O−M−O angles suggest that the geometry about the central metal atoms is slightly distorted from an octahedron. The sum of the neighboring O−M−O angles is, or is close to, 360°. The two platinum atoms within a cation sit above and below the coordination planes of MO_4 with Pt−M−Pt angles of 180° or nearly so. The cyclohexyl rings exhibit pseudo-coplanarity due to their disorder.

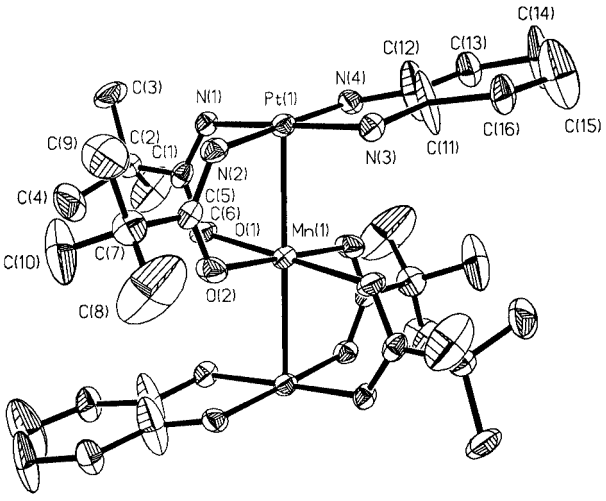

Figure 1. ORTEP plot of $[\{Pt(DACH)(\mu\text{-}NHCOtBu)_2\}_2Mn]^{2+}$ (**5**) with thermal ellipsoids plotted at 30% probability level

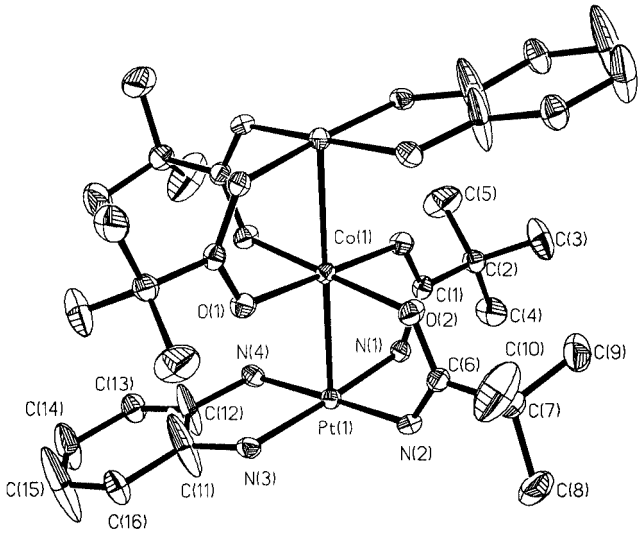

Figure 2. ORTEP plot of $[\{Pt(DACH)(\mu\text{-}NHCOtBu)_2\}_2Co]^{2+}$ (**6**) with thermal ellipsoids plotted at 30% probability level

The Pt−Mn distances [2.643(3) Å] of **5** are shorter than those found in $[\{Pt(NH_3)_2(\mu\text{-}MeT)_2\}_2Mn]^{2+}$ (MeT = 1-methylthymine) [2.704(1) Å], which has a similar Mn^{II} coordination geometry.[16] The Pt−Mn distances of **5** are also shorter than that in $[(dppe)(CH_3)PtMn(CO)_5]$ [2.795 Å] which contains a typical Pt−Mn covalent single bond.[17] The Pt−Cu distances in **7** are 2.6529(8) Å, which are shorter than that in both the PtCu dimer *cis*-$[(NH_3)_2Pt(1\text{-}MeU)_2Cu(H_2O)_2]^{2+}$ [2.756(3) Å] and the Pt_2Cu trimer *cis*-$[(NH_3)_2Pt(1\text{-}MeU)_2Cu(1\text{-}MeU)_2Pt(NH_3)_2]^{2+}$ [2.681(1) Å, 1-MeU = 1-methyluracilato],[18] and much shorter than those in the platinum−copper complexes bridged by alkynyl ligands.[19]

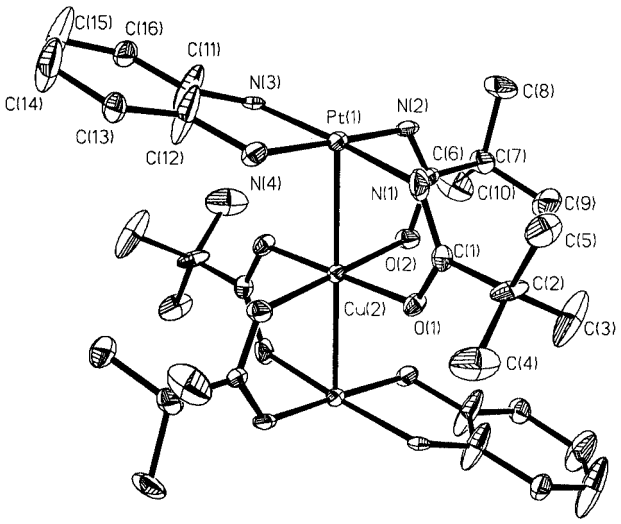

Figure 3. ORTEP plot of $[\{Pt(DACH)(\mu\text{-}NHCO\textit{t}Bu)_2\}_2Cu]^{2+}$ (**7**) with thermal ellipsoids plotted at 30% probability level

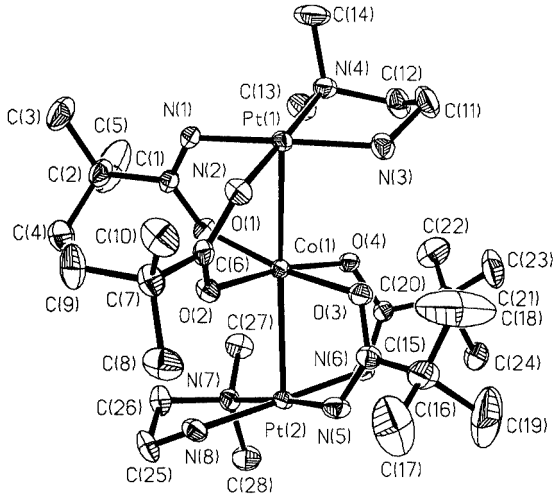

Figure 4. ORTEP plot of $[\{Pt(NH_2CH_2CH_2NMe_2)(\mu\text{-}NHCO\textit{t}Bu)_2\}_2Co]^{2+}$ (**13**) with thermal ellipsoids plotted at 30% probability level

The Pt−Co bonds of **13** [2.6902(10) and 2.6830(9) Å] are slightly longer than those of **6** [2.6087(6) Å] and **16** [2.6031(7) Å] because of the large steric hindrance of the NMe_2 groups. They are also longer than those in the Pt−Co clusters $[PtCo_2(CO)_7(cod)]$ [2.515(1) and 2.514(1) Å] and $[Pt_2Co_2(CO)_8(\mu_3\text{-}EtC_2Et)]$ [2.551(1) and 2.556(1) Å],[20] and in the $(Ph_2P)_2NH$-bridged Pt−Co carbonyl complexes [2.531(2)−2.508(2) Å],[21] indicating weak metal−metal interactions in the amidate-bridged platinum−cobalt complexes **6**, **13**, and **16**.

Structures of 8 and 14

When compound **2** was treated with Ni^{2+} in H_2O/acetone under the same conditions as for **5**−**7**, the expected product $[\{Pt(DACH)(\mu\text{-}NHCO\textit{t}Bu)_2\}_2Ni](ClO_4)_2$ was not obtained, but, instead, $[\{Pt(NH_3)(\mu\text{-}DACHCO\textit{t}Bu)(\mu\text{-}NHCO\textit{t}Bu)\}_2Ni](ClO_4)_2$ (**8**) was isolated in high yield as light green crystals, the structure of which was revealed by X-ray diffraction analysis (Figure 6). One of the two *t*BuCO groups shifts to the adjacent nitrogen atom of 1,2-diaminocyclohexane. This rearrangement is remarkable since the large *t*BuCO group and two hydrogen atoms have to exchange simultaneously. The most striking feature of compound **8** is that, although it has the same linear Pt−M−Pt arrangement, the two amidate bridging ligands are *trans* about the platinum atom. The Pt−Ni distance, 2.5750(14) Å, is slightly shorter than for the closely related trinuclear Pt_2Ni complex $[\{Pt(NH_3)_2(\mu\text{-}NHCO\textit{t}Bu)_2\}_2Ni](ClO_4)_2$.[6]

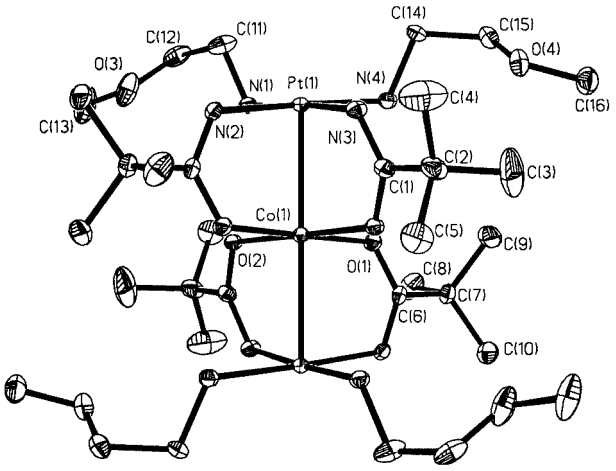

Figure 5. ORTEP plot of $[\{Pt(NH_2CH_2CH_2OCH_3)_2(\mu\text{-}NHCO\textit{t}Bu)_2\}_2Co]^{2+}$ (**16**) with thermal ellipsoids plotted at 30% probability level

Table 1. Important bond lengths [Å] and angles [°] of **5**−**9** and **11**−**17**

	M ion	Pt−M	Pt−M−Pt
5	Mn^{2+}	2.643(3)	180.0
6	Co^{2+}	2.6087(6)	180.0
7	Cu^{2+}	2.6529(8)	180.0
8	Ni^{2+}	2.5750(14)	179.48(17)
9	In^{3+}	2.6358(8)	180.0
11	In^{3+}	2.6422(6), 2.6278(6)	174.78(3)
12	Cd^{2+}	2.8156(9), 2.8196(9)	145.50(3)
13	Co^{2+}	2.6830(9), 2.6902(10)	168.13(2)
14	Ni^{2+}	2.6466(9), 2.6544(10)	169.33(2)
15	Zn^{2+}	2.5932(5)	180.0
16	Co^{2+}	2.6031(7)	180.0
17	Ag^{+}	2.8203(14), 2.8531(14), 2.9161(7)	167.52(6), 180.0

The rearrangement reaction is not generally seen, as illustrated by the isolation and characterization of $[\{Pt(NH_3)_2(\mu\text{-}NHCO\textit{t}Bu)_2\}_2Ni](ClO_4)_2$[6] and $[\{Pt(NH_2CH_2CH_2NMe_2)(\mu\text{-}NHCO\textit{t}Bu)_2\}_2Ni](ClO_4)_2$ (**14**). Both **14** and **15** are the expected Pt_2Ni products. The amine exchange reaction between a free amine and an acetamide is well known, unlike the migration of the BuCO group. It is not clear why such a rearrangement occurs only for complex **8**. The structure of **14** is shown in Figure 7. Because of the steric hindrance of the NMe_2 units, the Pt−Ni distances [2.6466(9), 2.6544(10) Å] of **14** are longer than those of **8**

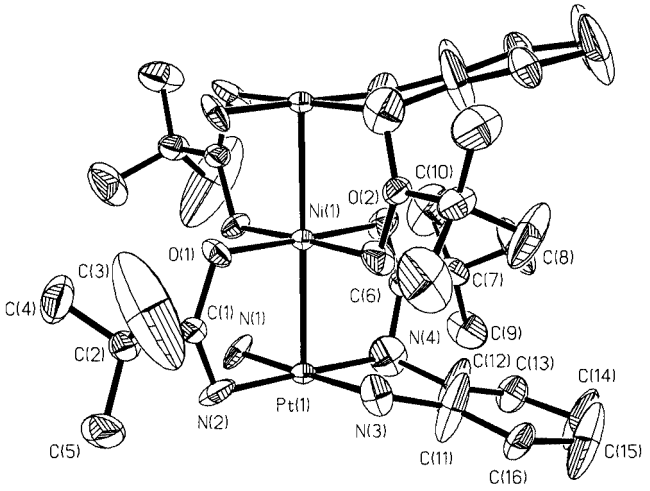

Figure 6. ORTEP plot of $[\{Pt(NH_3)(DACHCO\textit{t}Bu)(\mu\text{-}NHCO\textit{t}Bu)\}_2Ni]^{2+}$ (**8**) with thermal ellipsoids plotted at 30% probability level

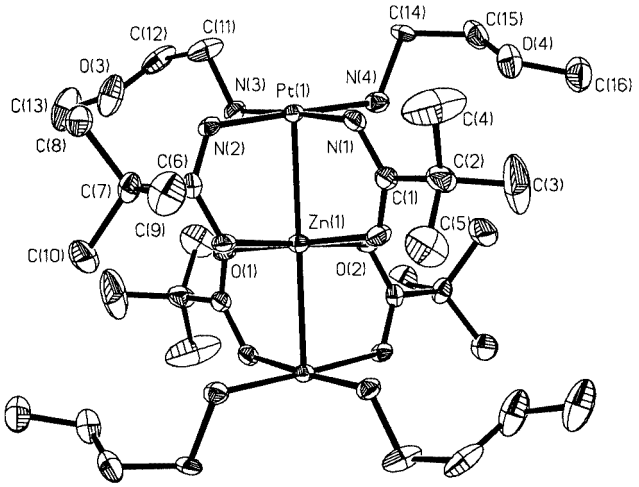

Figure 8. ORTEP plot of $[\{Pt(NH_2CH_2CH_2OCH_3)_2(\mu\text{-}NHCO\textit{t}Bu)\}_2Zn]^{2+}$ (**15**) with thermal ellipsoids plotted at 30% probability level

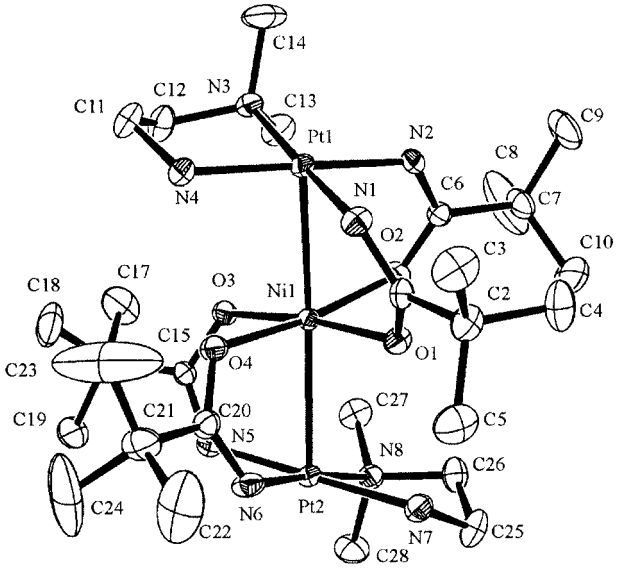

Figure 7. ORTEP plot of $[\{Pt(NH_2CH_2CH_2NMe_2)(\mu\text{-}NHCO\textit{t}Bu)\}_2Ni]^{2+}$ (**14**) with thermal ellipsoids plotted at 30% probability level

[2.5750(14) Å], and the Pt−Ni−Pt vector [169.33(2)°] is more bent.

Structure of 15

The trinuclear Pt_2Zn complex $[\{Pt(NH_2CH_2CH_2OMe)_2(\mu\text{-}NHCO\textit{t}Bu)_2\}_2Zn]^{2+}$ (**15**) was isolated as colorless crystals, and its structure is shown in Figure 8. Similar to other heteronuclear Pt_2M (M = Mn, Co, Ni, Cu) complexes, **15** contains a linear trimetallic core, in which Pt and Zn are doubly bridged by the amidate ligands. The methoxy groups remain uncoordinated. The Pt−Zn bond lengths are 2.5932(5) Å — comparable to the sum of covalent radii of the two metals (2.55 Å). Heteronuclear complexes containing direct Pt−Zn interaction have not been reported, but PtZn alloys are known catalysts for the dehydrogenation of alkanes.[22]

Structure of 12

The platinum−cadmium complex $[\{Pt(NH_3)_2(\mu\text{-}NHCO\textit{t}Bu)_2\}_2Cd]^{2+}$ (**12**) crystallizes in the space group $P2_1/n$. Its structure is shown in Figure 9. The platinum and cadmium centers are held together by four amidate ligands, which act as bridging units via their NCO groups. Unlike the analogous Pt_2Zn compound, the central Cd atom adopts tetrahedral geometry, which is completed by the four amidate oxygen atoms, or bicapped tetrahedron when the two rather long Pt−Cd contacts are also considered. The Pt−Cd distances [2.8156(9) and 2.8196(9) Å] are close to the sum of the metallic radii of platinum and cadmium (2.88 Å), indicating some Pt−Cd interaction. However, the Pt−Cd distances in **12** are much longer than the Pt−Cd dative bonds [2.6389(8) and 2.6101(8) Å] found in the complexes $[\{Pt(phpy)_2\}\{Cd(cyclen)\}](ClO_4)_2$ and

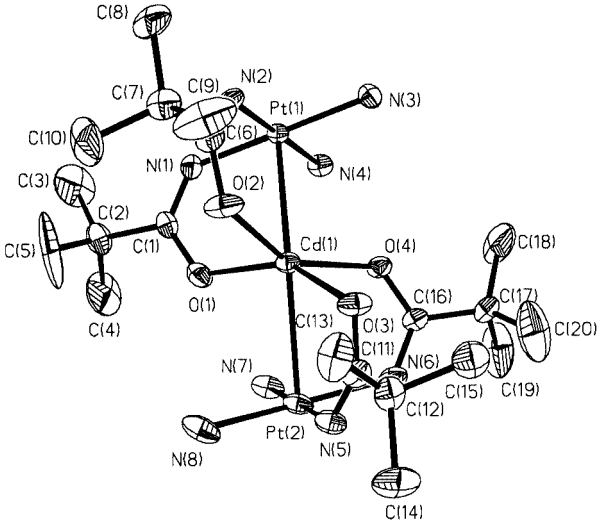

Figure 9. ORTEP plot of $[\{Pt(NH_3)_2(\mu\text{-}NHCO\textit{t}Bu)\}_2Cd]^{2+}$ (**12**) with thermal ellipsoids plotted at 30% probability level

[{$PtMe_2$(bipy)}{Cd(cyclen)}]$(ClO_4)_2$ (Hphpy = 2-phenylpyridine, bipy = 2,2′-bipyridine; cyclen = 1,4,7,10-tetraazacyclododecane).[23] Pt−Cd distances in **12** are much shorter than those in $(NBu_4)_2$[{Pt(μ-C≡CPh)$_4$}$_2$($CdCl_2$)] [2.960(1) Å][24] and [Pt_4Cd_6(C≡CPh)$_4$(μ-C≡CPh)$_{12}$(μ$_3$-OH)$_4$] [2.8570(14)−3.2234(8) Å].[25] The Pt−Cd−Pt is bent [145.50(3)°]. The Cd−O distances fall in the range 2.214(8)−2.263(9) Å, which are not unusual.[25]

Structures of 9 and 11

[{Pt(DACH)(μ-NHCO*t*Bu)$_2$}$_2$In]$^{3+}$ (**9**) crystallizes in a triclinic space group $P\bar{1}$, whereas [{Pt(NH_3)$_2$(μ-NHCO*t*Bu)$_2$}$_2$In]$^{3+}$ (**11**) crystallizes in a chiral orthorhombic space group $P2_12_12_1$. The indium(III) ions in both **9** and **11** are approximately octahedrally coordinated by four equatorial oxygen atoms of the amidate ligands, and two platinum atoms occupy the axial sites. The structures of **9** and **11** are shown in Figures 10 and 11, respectively. The indium atom and the four oxygen atoms are almost co-planar, with the sum of the neighboring O−In−O angles being 360°. The Pt−In bond lengths are 2.6358(8) Å for **9** and 2.6279(8) and 2.6412(8) Å for **11**. The Pt−In−Pt angle for **9** is 180°, whereas that of **11** (174.81°) deviates slightly from 180°. The two [Pt(RNH_2)$_2$($NHCOtBu$)$_2$] units maintain a square-planar geometry.

The In−O bonds of **9** [2.128(6)−2.167(6) Å] and **11** [2.128(6)−2.16786] Å] are only slightly longer than those in the indium alkoxide complexes [In(μ-OR)(OR)$_2$]$_2$ (R = *t*Bu, CMe_2Et, $CMeEt_2$, and CMe_2iPr) [1.985(4)−2.152(6) Å].[26] Platinum−indium heterometallic complexes containing Pt−In donor−acceptor interactions have been rarely studied. The Pt−In distances of **9** and **11** are similar to those in $LaPtIn_3$ (Pt−In, 2.694 Å),[27] [{$Cy_2P(CH_2CH_2)PCy_2$}Pt(InR_2)(R)] (R = CH_2SiMe_3, Pt−In, 2.601 Å),[28] but longer than those in [Pt{$InC(SiMe_3)_3$}$_4$] (2.441 Å).[29]

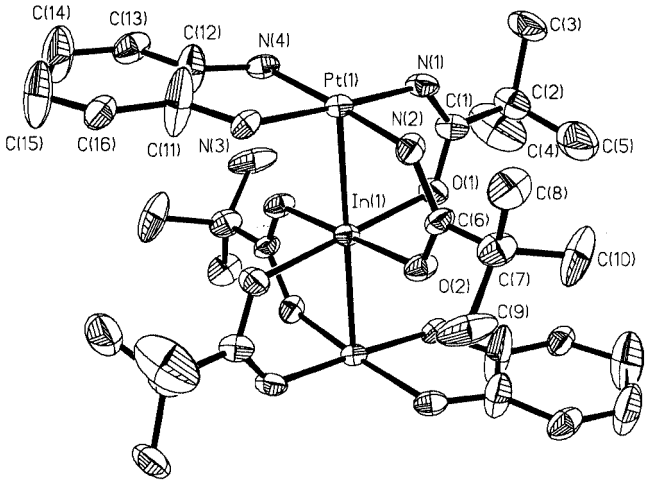

Figure 10. ORTEP plot of [{Pt(DACH)(μ-NHCO*t*Bu)$_2$}$_2$In]$^{3+}$ (**9**) with thermal ellipsoids plotted at 30% probability level

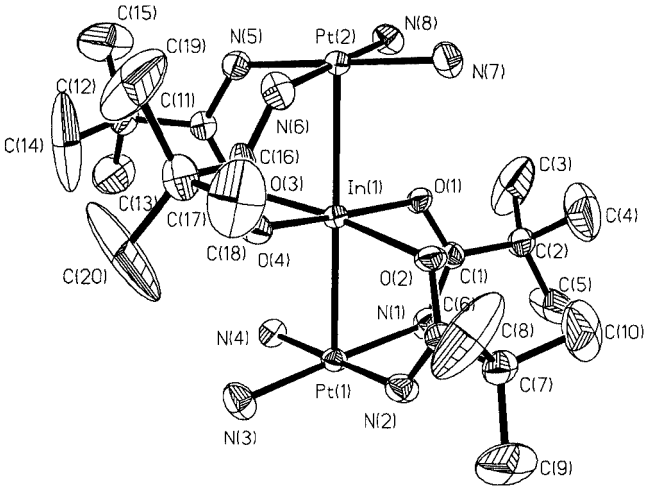

Figure 11. ORTEP plot of [{Pt(NH_3)$_2$(μ-NHCO*t*Bu)$_2$}$_2$In]$^{3+}$ (**11**) with thermal ellipsoids plotted at 30% probability level

Structure of 17

In the structure of the platinum−silver complex [{Pt($NH_2CH_2CH_2OCH_3$)$_2$(μ-NHCO*t*Bu)$_2$}$_4$$Ag_3$]$^{3+}$ (**17**) (Figure 12) the Pt_4Ag_3 cation is a chain of limited length, consisting of alternating Pt and Ag atoms bridged by amidate ligands. The metal−metal distances in the chain are 2.8203(14), 2.8531(14), and 2.9161(7) Å. There are two independent silver atoms, and Ag(2) is at the crystallographic inversion center. Ag(1) adopts a distorted trigonal-bipyramidal geometry with three amidate oxygen atoms at the equatorial positions and two Pt atoms occupying the two axial positions; the Pt(1)−Ag(1)−Pt(2) angle is 167.52(6)°. The coordination geometry around the Ag(2) atom is square-planar, and the Ag atom is linearly coordinated by two amidate oxygen and two Pt atoms, with a Pt(2)−Ag(2)−Pt(2a) angle of 180°. The Pt−Ag [2.8203(17), 2.8531(14), and 2.9161(7) Å] are close to those in other heteronuclear Pt−Ag complexes.[13] In contrast, the reaction

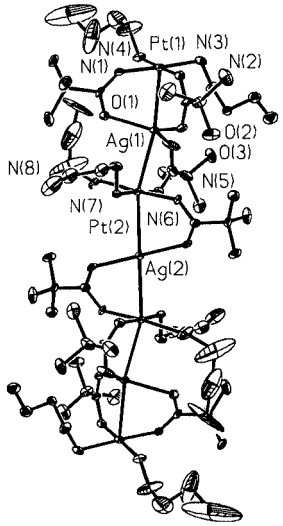

Figure 12. ORTEP plot of [{Pt($NH_2CH_2CH_2OCH_3$)-($NHCOtBu$)$_2$}$_4$$Ag_3$]$^{3+}$ (**17**) with thermal ellipsoids plotted at 30% probability level

of $AgNO_3$ with *trans*- and *cis*-$[Pt(NH_3)_2(NHCOMe)_2]$ yielded the heteronuclear polymeric complexes *cis*- and *trans*-$[(NH_3)_2Pt(NHCOMe)_2Ag]NO_3$, in which Pt and Ag atoms are all singly bridged by acetamidate ligands.[14]

Electrochemistry

Electrochemical data were obtained from freshly prepared nitrogen-purged DMSO, and CH_3CN, solutions of the trinuclear complexes, and for their parent platinum complexes. The cyclic voltammograms of all the compounds exhibit an irreversible oxidation, whose peak potentials in DMSO at 50 $mV \cdot s^{-1}$ are 0.50 ($[Pt(NH_3)_2(NHCOtBu)_2]$), 0.44 (**2**), ca. 0.48 (**3**), and 0.56 V (**4**) versus Fc/Fc^+. The electron-transfer behaviour of the trinuclear complexes **5**−**15** is essentially identical to that of the parent platinum complexes, which involve oxidation potentials in the range 0.41−0.49 V. Thus, the complexation of $[Pt(RNH_2)_2(NHCOtBu)_2]$ to a heterometal ions does not significantly change the platinum-based redox potentials. Obviously, metal−metal charge transfer is not important for these trinuclear complexes and the Pt−M interactions within **5**−**15** are very weak.

Conclusion

A number of amidate-bridged trinuclear complexes containing a trimetallic Pt−M−Pt core, either linear or bent, have been prepared in good yield by reactions between $[Pt(RNH_2)_2(NHCOtBu)_2]$ and the corresponding metal ions. The platinum units can bind heterometal ions through amidate oxygen atoms. The cyclic voltammograms, ^{195}Pt NMR spectra, and solid-state infrared spectra suggest that metal−metal interactions between platinum and the heterometals are limited. The short Pt−M distances of the Pt_2M (M = Mn, Co, Ni, Cu, Cd, Zn, and In) and Pt_4Ag_3 complexes, revealed by X-ray diffraction analyses, may be attributed to geometric requirement of the bridging amidate ligands, although attractions between the platinum and the heterometal ions could not be excluded. The two $[Pt(RNH_2)_2(NHCOtBu)_2]$ units and an M ion are held together mainly by the amidate functionality. The substituents on the amine ligands do not affect significantly the Pt−M interactions.

Experimental Section

General Remarks: $[Pt(NH_3)_2(NHCOtBu)_2]\cdot 2H_2O$[12] and $PtCl_2(DACH)$[30] were prepared according to the published procedure. All other chemicals were of A. R. grade and used as received. Elemental analyses were performed with a Perkin−Elmer PE 2400II analyzer. IR spectra as KBr pellets were recorded with a Perkin−Elmer 2000 spectrophotometer. ^1H and ^{195}Pt NMR spectra were recorded with a Bruker 500 MHz spectrometer. The NMR chemical shifts are given in ppm relative to TMS (^1H) and K_2PtCl_4 (^{195}Pt), and referenced either to residual solvent signals (^1H) or externally (^{195}Pt). UV/Vis spectra were recorded with a JASCO v-570 spectrophotometer. Cyclic voltammograms were obtained by use of a BAS CV-50 W instrument, in 10^{-5} M DMSO solutions containing 0.05 M $(Bu_4N)ClO_4$ as supporting electrolyte at a scan rate of 50 $mV \cdot s^{-1}$, and a three-electrode cell composed of an Ag/$AgNO_3$ reference electrode, a 3.0-mm glassy carbon working electrode, and a platinum counter electrode. The potentials were referenced to the ferrocenium/ferrocene couple.

$[Pt(DACH)(NCtBu)_2](ClO_4)_2\cdot H_2O$ (1): A suspension of $PtCl_2(DACH)$ (1.14 g, 3.0 mmol) in water (15 mL) was treated with $AgClO_4$ (1.24 g, 6.0 mmol), and the resultant mixture was stirred overnight in the dark. After removal of AgCl, *t*BuCN (1.0 g, 12.0 mmol) was added to the filtrate. The so-obtained white precipitate was then separated and washed with H_2O, EtOH, and Et_2O, and dried in air. Yield: 1.95 g (94%). $C_{16}H_{32}Cl_2N_4O_8Pt\cdot H_2O$ (692.45): calcd. C 27.75, H 4.95, N 8.09; found C 27.55, H 4.93, N 7.94. ^1H NMR (500 MHz, [D$_6$]acetone): δ = 1.20−2.75 (m, C_6H_{10}, 10 H), 3.01 (s, H_2O), 1.52 [s, $C(CH_3)_3$, 18 H] ppm. ^{195}Pt NMR (107.00 MHz, [D$_6$]acetone): δ = −2857.2 ppm.

$[Pt(DACH)(NHCOtBu)_2]\cdot 4H_2O$ (2): A suspension of **1** (1.45 g, 2.0 mmol) in water (10 mL) was treated with NaOH (0.20 g, 5.0 mmol). The resultant mixture was then stirred at room temperature overnight to give a white solid that was collected by filtration, washed with cold water, and dried in air. Yield: 1.12 g (96%). $C_{16}H_{34}N_4O_2Pt\cdot 4H_2O$ (581.61): calcd. C 33.04, H 7.28; N 9.63; found C 33.29, H 6.78, N 9.57. ^1H NMR (500 MHz, [D$_6$]DMSO): δ = 6.50, 4.65 (each d, $J_{H,H}$ = 9 Hz, NH_2, each 2 H), 5.59 (s, NH, 2 H), 3.38 (s, H_2O), 1.07 [s, $C(CH_3)_3$, 18 H], 2.21, 1.91, 1.51, 1.29, 1.10 (m, C_6H_{10}, each 2 H) ppm. ^{195}Pt (107.00 MHz, [D$_6$]DMSO): δ = −2625.2 ppm.

$[Pt(NH_2CH_2CH_2OCH_3)_2(NHCOtBu)_2]$ (3): This compound was isolated as a white hygroscopic solid according to the method described for **2**, but starting from $PtCl_2(NH_2CH_2CH_2OCH_3)_2$ (1.20 g, 2.0 mmol). Yield: 0.73 g (67%). $C_{16}H_{38}N_4O_4Pt$ (545.58): calcd. C 35.22, H 7.02, N 10.27; found C 34.89, H 7.46, N 9.72.

$[Pt(NH_2CH_2CH_2NMe_2)(NHCOtBu)_2]$ (4): As described for **3**, but starting from $PtI_2(NH_2CH_2CH_2NMe_2)$ (0.54 g, 1.0 mmol), compound **4** was isolated as a white hygroscopic solid. Yield: 0.20 g (42%). $C_{14}H_{32}N_4O_2Pt$ (483.51): calcd. C 34.78, H 6.67, N 11.59; found C 33.26, H 7.02, N 11.12; the elemental analysis is unsatisfactory due to the compound's hygroscopic properties. ^1H NMR (270.05 MHz, [D$_6$]acetone): δ = 5.21 (s, NH_2, 2 H), 4.89, 4.63 (both s, NH, each 1 H), 2.92, 2.74 (both t, CH_2, $J_{H,H}$ = 6.0 Hz, each 2 H), 2.83 [s, $N(CH_3)_2$, 6 H], 1.15, 1.05 [both s, $C(CH_3)_3$, each 9 H] ppm. ^{195}Pt (57.95 MHz, [D$_6$]DMSO): δ = −2657 ppm.

$[\{Pt(DACH)(\mu\text{-}NHCOtBu)_2\}_2Mn](ClO_4)_2\cdot 2(CH_3)_2CO$ (5): $[Pt(DACH)(NHCOtBu)_2]\cdot 4H_2O$ (58 mg, 0.10 mmol) in acetone (2 mL) was added to a solution of $MnCl_2\cdot 4H_2O$ (20 mg, 0.10 mmol) and $NaClO_4$ (50 mg) in water (2 mL). Pale-yellow crystals were grown by slow concentration of the resultant solution. Yield: 57 mg (81%). $C_{32}H_{68}Cl_2N_8O_{12}Pt_2Mn\cdot 2(CH_3)_2CO$ (1389.09): calcd. C 32.86, H 5.80, N 8.07; found C 32.73; H 5.91, N 7.94.

$[\{Pt(DACH)(\mu\text{-}NHCOtBu)_2\}_2Co](ClO_4)_2\cdot 2(CH_3)_2CO$ (6): This compound was prepared in a similar manner to **5** except that $Co(NO_3)_2\cdot 6H_2O$ (29 mg, 0.10 mmol) was used in place of $MnCl_2\cdot 4H_2O$. Yield: 60 mg (86%). $C_{32}H_{68}Cl_2N_8O_{12}Pt_2Co\cdot 2(CH_3)_2CO$ (1393.08): calcd. C 32.76, H 5.79, N 8.04; found C 32.94; H 6.02; N 7.87.

$[\{Pt(DACH)(\mu\text{-}NHCOtBu)_2\}_2Cu](ClO_4)_2$ (7): The method employed for compound **5** was used to prepare **7**, except that $Cu(ClO_4)_2\cdot 6H_2O$ (37 mg, 0.10 mmol) was used in place of

$MnCl_2·4H_2O$. Yield: 52.5 mg (82%). $C_{32}H_{68}Cl_2N_8O_{12}Pt_2Cu$ (1281.54): calcd. C 29.99, H 5.35, N 8.74; found C 30.03, H 5.15, N 8.67.

[{Pt(NH$_3$)(μ-DACHCO*t*Bu)(μ-NHCO*t*Bu)}$_2$Ni](ClO$_4$)$_2$ (8): Compound **8** was prepared in a similar manner as for **5** except that $Ni(NO_3)_2·6H_2O$ (29 mg, 0.10 mmol) was used instead of $MnCl_2·4H_2O$. Yield: 54 mg (84%). $C_{32}H_{68}Cl_2N_8O_{12}Pt_2Ni$ (1276.68): calcd. C 30.10, H 5.37, N 8.78; found C 30.06; H 5.35; N 8.66.

[{Pt(DACH)(μ-NHCO*t*Bu)$_2$}$_2$In](ClO$_4$)$_3$ (9): Here the method used to synthesize **5** was employed, with $In(NO_3)_3·6H_2O$ (41 mg, 0.10 mmol) in place of $MnCl_2·4H_2O$, to give **9** in 63% yield (45 mg). $C_{32}H_{68}Cl_3N_8O_{16}Pt_2In$ (1432.26): calcd. C 26.83, H 4.79, N 7.82; found C 26.79, H 4.68, N 7.68. ^{1}H NMR (500 MHz, [D$_6$]DMSO): δ = 6.85, 6.01 (both d, $J_{H,H}$ = 9.0 Hz, NH_2, each 2 H), 6.33, 6.30 (both s, NH, each 2 H), 5.70, 4.44 (both t, $J_{H,H}$ = 9.0 Hz, each 2 H), 1.01−2.72 (m, C_6H_{10}, 20 H), 1.12 [s, $C(CH_3)_3$, 36 H] ppm. ^{195}Pt (107.00 MHz, [D$_6$]DMSO): δ = −2439 ppm.

[{Pt(DACH)(μ-NHCO*t*Bu)$_2$}$_2$Cd](ClO$_4$)$_2$ (10): Compound **10** was prepared in a similar manner as for **3**, starting from $CdSO_4·6H_2O$ (32 mg, 0.10 mmol). Yield: 51 mg (76%). $C_{32}H_{68}Cl_2N_8O_{12}Pt_2Cd$ (1330.4): calcd. C 28.89, H 5.15, N 8.42; found C 28.45, H 5.30, N 8.36. ^{1}H NMR (500 MHz, [D$_6$]DMSO): δ = 6.06, 5.55, 5.38, 4.60 (all s, NH_2, each 2 H), 5.57, 5.41 (both s, NH, each 2 H), 1.40−2.73 (m, C_6H_{10}, 20 H), 1.13, 1.04 [both s, $C(CH_3)_3$, each 18 H] ppm. ^{195}Pt (107.00 MHz, [D$_6$]DMSO): δ = −2562 ppm.

[[Pt(NH$_3$)$_2$(NHCO*t*Bu)$_2$]$_2$In](ClO$_4$)$_3$·C$_3$H$_6$O (11): $[Pt(NH_3)_2(NHCOtBu)_2]·2H_2O$ (47 mg, 0.10 mmol) was added to a solution of $In(NO_3)_3·6H_2O$ (41 mg, 0.10 mmol) in H_2O (2 mL). The resultant colorless solution yielded a colorless precipitate immediately after subsequent addition of $NaClO_4$. Cooling at 5 °C overnight gave colorless crystals, which were filtered off and then washed with cold water, EtOH, and Et_2O. Yield: 53 mg (79%). $C_{20}H_{52}Cl_3InN_8O_{16}Pt_2·(CH_3)_2CO$ (1330.08): calcd. C 20.77, H 4.40, N 8.42; found C 20.39, H 4.25, N 8.58. ^{1}H NMR (500.00 MHz, [D$_6$]DMSO): δ = 6.46 (s, NH, 2 H), 4.13 (s, NH_3, 6 H), 2.07 [s, $(CH_3)_2CO$, 6 H), 1.10 [s, $C(CH_3)_3$, 18 H] ppm. ^{195}Pt NMR (107.30 MHz, [D$_6$]DMSO): δ = −2474 ppm.

[{Pt(NH$_3$)$_2$(μ-NHCO*t*Bu)$_2$}$_2$Cd](ClO$_4$)$_2$·2H$_2$O (12): This compound was obtained similarly to **11** by using the corresponding materials $Cd(NO_3)_2·4H_2O$ (24 mg, 0.10 mmol), $NaClO_4$ (50 mg, 0.43 mmol), and $[Pt(NH_3)_2(NHCOtBu)_2]·2H_2O$ (47 mg, 0.10 mmol). Yield: 51 mg (84%). $C_{20}H_{52}CdCl_2N_8O_{12}Pt_2·2H_2O$ (1206.18): calcd. C 19.92, H 4.68, N 9.29; found C 19.79, H 4.83, N 9.20. ^{1}H NMR (500.00 MHz, [D$_6$]DMSO): δ = 5.42 (br. NH_3, 12 H), 4.51 (br. NH, 4 H), 1.06 [s, $C(CH_3)_3$, 36 H] ppm. ^{195}Pt NMR (107.30 MHz, [D$_6$]DMSO): δ = −2561 ppm.

[{Pt(NH$_2$CH$_2$CH$_2$NMe$_2$)(μ-NHCO*t*Bu)$_2$}$_2$Co](ClO$_4$)$_2$·H$_2$O (13): Compound **13** was prepared by an analogous procedure to that of **6** but using **4** (48 mg, 0.10 mmol) and $Co(NO_3)_2·6H_2O$ (29 mg, 0.10 mmol) to isolate **13** as a blue solid. Yield: 50 mg (81%). $C_{28}H_{64}CoCl_2N_8O_{12}Pt_2·H_2O$ (1242.86): calcd. C 27.06, H 5.35, N 9.02; found C 27.30, H 5.30, N 9.20.

[{Pt(NH$_2$CH$_2$CH$_2$NMe$_2$)(μ-NHCO*t*Bu)$_2$}$_2$Ni](ClO$_4$)$_2$·H$_2$O (14): By a similar procedure to that used for **13**, but using $Ni(NO_3)_2·6H_2O$ (29 mg, 0.10 mmol), **14** was isolated as a green solid. Yield: 53 mg (86%). $C_{28}H_{64}Cl_2N_8NiO_{12}Pt_2·H_2O$ (1242.62): calcd. C 27.06, H 5.35, N 9.02; found C 26.93, H 5.47, N 8.96.

[{Pt(NH$_2$CH$_2$CH$_2$OCH$_3$)$_2$(μ-NHCO*t*Bu)$_2$}$_2$Zn](ClO$_4$)$_2$ (15): This compound was prepared as described for **5** but starting from **3** (55 mg, 0.10 mmol) and $Zn(ClO_4)_2·6H_2O$ (37 mg, 0.10 mmol), and was isolated as a white solid. Yield: 52 mg (76%). $C_{32}H_{76}Cl_2N_8O_{16}Pt_2Zn$ (1355.4): calcd. C 28.36, H 5.65, N 8.27; found C 28.34, H 5.42, N 8.05.

[{Pt(NH$_2$CH$_2$CH$_2$OCH$_3$)(μ-NHCO*t*Bu)$_2$}$_2$Co](ClO$_4$)$_2$ (16): Using the method described for **5**, but starting from **3** (55 mg, 0.10 mmol) and $Co(NO_3)_2·6H_2O$ (29 mg, 0.10 mmol), **16** was isolated as a blue solid in 78% yield (53 mg). $C_{32}H_{76}Cl_2CoN_8O_{16}Pt_2$ (1348.98): calcd. C 28.49, H 5.68, N 8.31; found C 28.22, H 5.79, N 8.20.

[{Pt(NH$_2$CH$_2$CH$_2$OCH$_3$)(NHCO*t*Bu)$_2$}$_4$Ag$_3$](ClO$_4$)$_3$·2H$_2$O (17): Compound **17** was prepared from **3** (55 mg, 0.10 mmol) and an equimolar amount of $AgClO_4$ (21 mg, 0.10 mmol) in water. Slow concentration of the resultant colorless solution yielded colorless crystals. Yield: 44 mg (63%). $C_{64}H_{152}Ag_3Cl_3N_{16}O_{28}Pt_4·2H_2O$ (2840.3): calcd. C 27.06, H 5.54, N 7.89; found C 26.82, H 5.63, N 7.45.

Table 2. Crystal data and structure refinement for compounds **5**−**9**, **17**

	5	**6**	**7**	**8**	**9**	**17**
Empirical formula	$C_{38}H_{80}Cl_2MnN_8O_{14}Pt_2$	$C_{38}H_{80}Cl_2CoN_8O_{14}Pt_2$	$C_{32}H_{68}Cl_2CuN_8O_{12}Pt_2$	$C_{32}H_{68}Cl_2N_8NiO_{12}Pt_2$	$C_{34}H_{74}Cl_3InN_8O_{17}Pt_2$	$C_{64}H_{152}Ag_3Cl_3N_{16}O_{28}Pt_4$
Formula mass	1389.12	1393.11	1281.56	1276.73	1478.33	2804.34
Crystal system	monoclinic	monoclinic	monoclinic	monoclinic	triclinic	monoclinic
Space group	$P2_1/c$	$P2_1/c$	$P2_1/n$	$C2$	$P\bar{1}$	$P2_1/n$
a [Å]	11.367(13)	11.273(3)	12.181(4)	21.847(12)	12.998(4)	14.235(4)
b [Å]	19.51(2)	19.415(5)	12.056(4)	11.883(7)	13.148(4)	24.889(6)
c [Å]	12.897(16)	12.888(3)	16.454(5)	11.302(6)	17.925(5)	16.097(4)
α [°]	90	90	90	90	74.715(5)	90
β [°]	100.88(2)	101.055(4)	93.753(6)	121.124(8)	79.638(5)	94.982(5)
γ [°]	90	90	90	90	73.405(5)	90
V [Å^3]	2809(6)	2768.5(13)	2411.1(14)	2512(2)	2813.7(14)	5682(3)
Z	2	2	2	2	2	2
$D_{calcd.}$ [Mg/m^3]	1.643	1.671	1.765	1.688	1.704	1.639
Refls. collected	16455	16689	14886	7444	14102	32411
Refls. unique	6226 (0.1854)	6157 (0.069)	5506 (0.0489)	9934 (0.0319)	10052 (0.0598)	12446 (0.0932)
GOF	0.959	1.193	1.475	1.043	0.957	1.066
$R1$, $wR2$ [$I > 2\sigma(I)$]	0.0626, 0.1370	0.0399, 0.0954	0.0653, 0.1417	0.0251, 0.0684	0.0580, 0.1337	0.0958, 0.2520
$R1$, $wR2$ (all data)	0.1208, 0.1562	0.0463, 0.0977	0.0765, 0.1446	0.0291, 0.0712	0.1087, 0.1478	0.1416, 0.2810

Table 3. Crystallographic data and structure refinement for compounds **11**−**16**

	11	**12**	**13**	**14**	**15**	**16**
Empirical formula	$C_{23}H_{58}Cl_3InN_8O_{17}Pt_2$	$C_{20}H_{56}CdCl_2N_8O_{14}Pt_2$	$C_{28}H_{66}Cl_2CoN_8O_{13}Pt_2$	$C_{28}H_{66}Cl_2N_8NiO_{13}Pt_2$	$C_{32}H_{76}Cl_2N_8O_{16}Pt_2Zn$	$C_{32}H_{76}Cl_2CoN_8O_{16}Pt_2$
Formula mass	1330.12	1206.21	1242.90	1242.68	1355.46	1349.02
Crystal system	orthorhombic	monoclinic	monoclinic	monoclinic	orthorhombic	orthorhombic
Space group	$P2_12_12_1$	$P2_1/n$	$P2_1/n$	$P2_1/n$	*Pbca*	*Pbca*
a [Å]	10.9233(9)	13.656(3)	12.878(5)	12.906(6)	14.067(2)	14.054(4)
b [Å]	18.5229(16)	19.988(5)	16.048(7)	16.144(7)	18.615(3)	18.491(5)
c [Å]	22.5474(19)	15.154(4)	21.637(9)	21.624(10)	20.106(3)	19.977(6)
β [°]	90	92.010(4)	98.644(7)	99.075(8)	90	90
V [Å^3]	4562.0(7)	4133.7(16)	4421(3)	4449(3)	5265.0(16)	5192(3)
Z	4	4	4	4	4	4
$D_{calcd.}$ [g/cm^3]	1.937	1.938	1.867	1.855	1.710	1.726
Refls. collected	28711	25791	27147	25851	29970	28599
Refls. uniqe (R_{int})	10434 (0.0850)	9391 (0.1313)	9966 (0.0312)	9934 (0.0319)	5969 (0.1092)	5821 (0.0585)
Goodness-of-fit	1.023	0.995	1.039	1.043	0.927	0.938
*R*1, *Rw* [$I > 2\sigma(I)$]	0.0435, 0.1002	0.0669, 0.1680	0.0272, 0.0631	0.0289, 0.0638	0.0427, 0.0908	0.0361, 0.0771
*R*1, *Rw* (all data)	0.0535, 0.1048	0.0901, 0.1841	0.0409, 0.0690	0.0481, 0.0712	0.1073, 0.1122	0.0717, 0.0935

X-ray Crystallographic Study: Data collection was performed with a Bruker Smart-CCD diffractometer using monochromatized Mo-K_α radiation, λ = 0.71073 Å, at room temperature. Data reduction was performed using SAINT+ Version 6.02 software.[31] The data were corrected for absorption by using the program SADBAS within the SAINTPLUS package. Structures were solved by the direct method. This solution yielded metal atoms, N, O, and some C atoms. Subsequent Fourier synthesis gave the remaining C-atom positions. The hydrogen atoms were geometrically fixed and allowed to ride on their attached atoms, and refined with the XSHELL software.[32] The final refinement included anisotropic thermal parameters for all of the non-hydrogen atoms and converged to the *R*1 and *wR*2 values listed in Tables 2 and 3. The crystal data collection and refinement parameters are summarized in Tables 2 and 3. CCDC-187851 (**5**), -187852 (**6**), -187853 (**7**), -187854 (**8**), -187855 (**9**), -188637 (**11**), -188638 (**12**), -195593 (**13**), -195594 (**14**), -195595 (**15**), -195596 (**16**), and -195597 (**17**) contain the supplementary crystallographic data for this paper. These data can be obtained free of charge at www.ccdc.cam.ac.uk/conts/retrieving.html [or from the Cambridge Crystallographic Data Centre, 12 Union Road, Cambridge CB2 1EZ, UK; Fax: (internat.) + 44-1223/336-033; E-mail: deposit@ccdc.cam.ac.uk].

[1] T. Tanase, R. A. Begum, H. Toda, Y. Yamamoto, *Organometallics* **2001**, *20*, 968−979.
[2] H. Song, Z. Zhang, Z. Hui, C. Che, T. C. W. Mak, *Inorg. Chem.* **2002**, *41*, 3146−3154.
[3] R. Clerac, F. A. Cotton, K. R. Dunbar, T. B. Lu, C. A. Murillo, X. P. Wang, *J. Am. Chem. Soc.* **2000**, *122*, 2272−2278.
[4] A. L. Balch, V. J. Catalano, M. M. Olmstead, *J. Am. Chem. Soc.* **1990**, *112*, 2010−2011.
[5] H. Xiao, Y. Weng, W. Wong, T. C. W. Mak, C. Che, *J. Chem. Soc., Dalton Trans.* **1997**, 221−226.
[6] W. Chen, K. Matsumoto, *Eur. J. Inorg. Chem.* **2002**, 2664−2670.
[7] J. R. Berenguer, J. Forniés, J. Gómez, E. Lalinde, M. T. Moreno, *Organometallics* **2001**, *20*, 4847−4851.
[8] J. K. Nagle, A. L. Balch, M. M. Olmstead, *J. Am. Chem. Soc.* **1988**, *110*, 319−321.
[9] A. L. Balch, S. P. Rowley, *J. Am. Chem. Soc.* **1990**, *112*, 6139−6140.
[10] P. Pyykkö, *Chem. Rev.* **1997**, *97*, 597−636.
[11] [11a] Y. Lin, S. Takeda, K. Matsumoto, *Organometallics* **1999**, *18*, 4897−4899. [11b] Y. Lin, H. Misawa, K. Matsumoto, *J. Am. Chem. Soc.* **2001**, *123*, 569−575. [11c] K. Matsumoto, J. Matsunami, K. Mizuno, H. Uemura, *J. Am. Chem. Soc.* **1996**, *118*, 8959−8960. [11d] K. Matsumoto, Y. Nagai, J. Matsunami, K. Mizuno, T. Abe, R. Somazawa, J. Kinoshita, H. Shimura, *J. Am. Chem. Soc.* **1998**, *120*, 2900−2907.
[12] W. Chen, K. Matsumoto, *Inorg. Chim. Acta* **2002**, *342*, 88−96.
[13] [13a] F. Zamora, H. Witkowski, E. Freisinger, J. Muller, B. Thormann, A. Albinati, B. Lippert, *J. Chem. Soc., Dalton Trans.* **1999**, 175−182. [13b] D. Holthenrich, M. Krumm, E. Zangrando, F. Pichierri, L. Randaccio, B. Lippert, *J. Chem. Soc., Dalton Trans.* **1995**, 3275−3279.
[14] A. Erxleben, B. Lippert, *J. Chem. Soc., Dalton Trans.* **1996**, 2329−2333.
[15] J. Arpalahti, K. D. Klika, S. Molander, *Eur. J. Inorg. Chem.* **2000**, 1007−1013.
[16] B. Lippert, U. Schubert, *Inorg. Chim. Acta* **1981**, *56*, 15−20.
[17] S. Komiya, S. Muroi, M. Furuya, M. Hirano, *J. Am. Chem. Soc.* **2000**, *122*, 170−171.
[18] B. Lippert, U. Thewalt, H. Schoellhorn, D. M. L. Goodgame, R. W. Rollins, *Inorg. Chem.* **1984**, *23*, 2807−2813.
[19] [19a] V. W. W. Yam, K. L. Yu, K. K. Cheung, *J. Chem. Soc., Dalton Trans.* **1999**, 2913−2915. [19b] J. P. H. Charmant, J. Forniés, J. Gomez, E. Lalinde, R. I. Merino, M. T. Moreno, A. C. Orpen, *Organometallics* **1999**, *18*, 3353−3358.
[20] R. D. Adams, G. Chen, W. G. Wu, J. G. Yin, *Inorg. Chem.* **1990**, *29*, 4208−4214.
[21] [21a] I. Bachert, I. Bartusseck, P. Braunstein, E. Guillon, J. Rose, G. Kickelbick, *J. Organomet. Chem.* **1999**, *588*, 144−151. [21b] I. Bachert, I. Bartusseck, P. Braunstein, E. Guillon, J. Rose, G. Kickelbick, *J. Organom. Chem.* **1999**, *580*, 257−264.
[22] J. Silvestre-Albero, M. A. Sanchez-Castillo, R. He, A. Sepulveda-Escribano, F. Rodriguez-Reinoso, J. A. Dumesic, *Catal. Lett.* **2001**, *74*, 17−25.
[23] T. Yamaguchi, F. Yamazaki, T. Ito, *J. Am. Chem. Soc.* **1999**, *121*, 7405−7406.
[24] J. P. H. Charmant, L. R. Falvello, J. Forniés, J. Gómez, E. Lalinde, M. T. Moreno, A. G. Orphen, A. Rueda, *Chem. Commun.* **1999**, 2045−2046.
[25] J. Forniés, J. Gómez, E. Lalinde, M. T. Moreno, *Inorg. Chem.* **2001**, *40*, 5415−5419.
[26] [26a] S. Suh, D. M. Hoffman, *J. Am. Chem. Soc.* **2000**, *122*, 9396−9404. [26b] T. J. Trentler, S. C. Goel, K. M. Hickman, A. M. Viano, M. Y. Chiang, A. M. Beatty, P. C. Gibbons, W. E. Buhro, *J. Am. Chem. Soc.* **1997**, *119*, 2172−2181.

[27] Y. V. Galadzhun, R. Pottgen, *Z. Angorg. Allg. Chem.* **1999**, *625*, 481−487.
[28] R. A. Fischer, J. Behm, *J. Organomet. Chem.* **1991**, *413*, C10−C14.
[29] W. Uhl, S. Melle, *Z. Anorg. Allg. Chem.* **2000**, *626*, 2043−2045.
[30] A. H. Talebian, D. Bensely, A. Ghiorghis, C. F. Hammer, P. S. Schein, D. Green, *Inorg. Chim. Acta* **1991**, *179*, 281−287.
[31] G. M. Sheldrick, *SHELXS-97, Program for X-ray Crystal Structure Solution*, University of Göttingen, Göttingen, Germany, **1997**.
[32] G. M. Sheldrick, *SHELXL-97, Program for X-ray Crystal Structure Refinement*, University of Götingen, Götingen, Germany, **1997**.

Received December 13, 2002
Early View Article
Published Online October 22, 2003

